Organic & Biomolecular Chemistry

Hydroboration of vinylsilanes providing diversity-oriented hydrophobic building blocks for biofunctional molecules

Journal:	*Organic & Biomolecular Chemistry*
Manuscript ID	OB-ART-04-2024-000632.R1
Article Type:	Paper
Date Submitted by the Author:	22-May-2024
Complete List of Authors:	Namba, Nao; Tokyo Medical and Dental University Fujii, Shinya; Tokyo Medical and Dental University, Institute of Biomaterials and Bioengineering

ARTICLE

Hydroboration of vinylsilanes providing diversity-oriented hydrophobic building blocks for biofunctional molecules

Received 00th January 20xx,
Accepted 00th January 20xx

DOI: 10.1039/x0xx00000x

Nao Namba[a] and Shinya Fujii*[a]

Hydroboration of vinylsilanes with BH_3 affords two silylethanol regioisomers. Here, we investigated the regioisomeric ratio of hydroboration products from various vinylsilanes, focusing on the characteristic reaction profile. All investigated vinylsilanes afforded both regioisomers, and greater bulkiness increased the proportion of Markovnikov products. The obtained silylethanols were used as hydrophobic building blocks for constructing nuclear progesterone receptor (PR) modulators. Notably, structural conversion from α-isomer (silylethan-1-oxy derivative) to β-isomer (2-silylethoxy derivative) caused complete activity-switching from PR agonist to antagonist. Our results indicate that silylethanols are useful for structural development, and vinylsilanes are a versatile source of hydrophobic building blocks for biofunctional molecules.

Introduction

Silicon functionalities are often utilized as reactants for coupling reactions or as protective groups. From the viewpoint of synthetic methods, organosilicon reagents offer a number of advantages: (1) silyl functionalities themselves can act as reactive sites for Hiyama coupling or Tamao-Fleming oxidation; (2) silyl groups are readily removable by acids or fluoride reagents; (3) the electronic effect of the silicon atom can produce characteristic regioselectivity; (4) the bulkiness of silyl substituents can provide characteristic regio- and stereoselectivity.[1] Therefore, many researchers use silyl reagents for the synthesis of natural products or functional molecules, including oligomers.[2,3] Vinylsilanes, which are organosilicon reagents bearing a vinyl group on the silicon atom, are intrinsically non-toxic, stable in air and also stable in aqueous solution. As they can react at the silicon atom or the unsaturated bond, they are useful for generating functional molecules. The silyl moiety also affords a characteristic reaction selectivity. For example, in the hydroboration of vinylsilanes with BH_3, the regioselectivity between Markovnikov products (α-isomers) and anti-Markovnikov products (β-isomers) is essentially different from that in the case of the corresponding vinyl hydrocarbons.[4,5] With trimethylvinylsilane (TMS ethylene), two products are obtained almost in 1:1 regioselectivity, whereas hydroboration of the corresponding hydrocarbon favors the anti-Markovnikov product (Fig. 1A). Taking advantage of these characteristics of vinylsilanes, several reactions have been developed and utilized. For example, Meng and coworkers developed site-selective, asymmetric hydroboration of vinylsilanes and utilized it in a total synthesis of bruguierol A.[6] However, in most cases, silyl moieties are employed only as leaving or protecting groups to be eventually removed.

In the field of drug discovery, on the other hand, the introduction of functionalities containing different elements is a promising approach to develop novel and distinctive candidates.[7]

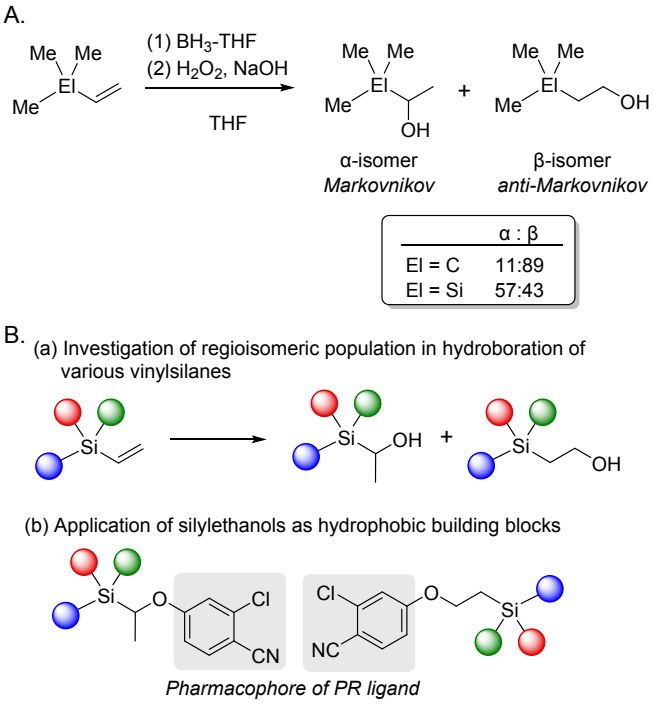

Fig. 1. A) Regioisomeric ratio in the hydroboration of *tert*-butylethene and trimethylsilylethene, reported by Soderquist and Bailey. B) Objectives of this research.

[a] *Institute of Biomaterials and Bioengineering, Tokyo Medical and Dental University, 2-3-10 Kanda-Surugadai, Chiyoda-ku, Tokyo 101-0062, Japan.*

Electronic Supplementary Information (ESI) available: synthesis of vinylsilanes, detail of DFT calculation, synthetic procedures, and compound characterization. See DOI: 10.1039/x0xx00000x

In this context, the silicon atom has a longer covalent bond length than carbon, and so the hydrophobic surface of a molecule can be extended by introducing a silyl moiety. It is already established that "Si/C-exchange" is a good strategy to improve biological activity and target selectivity, as well as the pharmacokinetic profile.[8-11] Focusing on the availability and diversity of silyl reagents, we previously developed a silyl group-based structural development strategy for hydrophobic substructures,[12] and reported the development of nuclear receptor modulators with unique target-selectivity profiles.[13-16] Thus, we anticipated that the hydroboration products of vinylsilanes could prove to be useful hydrophobic building blocks for biofunctional compounds. In particular, we noted that hydroboration of vinylsilanes and subsequent oxidation can afford two products, i.e. 1-silylethanols (α-isomers) and 2-silylethanols (β-isomers), and therefore this reaction could be especially suitable for the preparation of diversity-oriented hydrophobic building blocks. Based on these considerations, we first set out to investigate the regioisomeric ratio of hydroboration products using a wide variety of vinylsilanes as substrates. We then investigated the application of the resulting hydroboration products as hydrophobic building blocks of nuclear progesterone receptor (PR) ligands (Fig. 1B).

Results and discussion

Hydroboration of vinylsilanes

First, we prepared vinylsilanes **1a**-**1m** bearing various kinds of alkyl or aryl moiety using several known methods (Scheme S1) and conducted hydroboration reactions. Table 1 summarizes the regioisomeric ratio of the reaction products and the isolated yield of each isomer of the obtained silylethanols (Table 1). In all cases (**1a**-**1m**), hydroboration using BH_3-THF gave two silylethanols **2a**-**2m** and **3a**-**3m** simultaneously. The sum of the isolated yields of silylethanols **2b** and **3b** was only moderate due to the difficulty of purification on a laboratory (milligram) scale. Notably, hydroboration of **1c** using BH_3-Me_2S gave the two isomers in a similar ratio to that in the case of BH_3-THF, suggesting that the characteristic regio-nonselectivity in the hydroboration of vinylsilanes using BH_3 has generality. In contrast, hydroboration of **1c** using 9-BBN gave only 2-silylethanol (β-isomer) **3c**. In the case of hydroboration with BH_3, the regioisomeric ratio of products was in the range between 55:45 and 71:29, and the major product was always 1-silylethanol (α-isomer) **2**. Interestingly, the ratio of the sterically unfavorable product **2** increased with increasing bulkiness of the silyl substituent. Specifically, replacing the three methyl groups with ethyl or phenyl groups changed the regioselectivity from 58:42 to 61:39 or 71:29 (**1a** vs **1b**, **1e**), respectively.

Table 1. Regioisomeric ratio and isolated yield of hydroboration products from vinylsilanes **1a**-**1m**.[a]

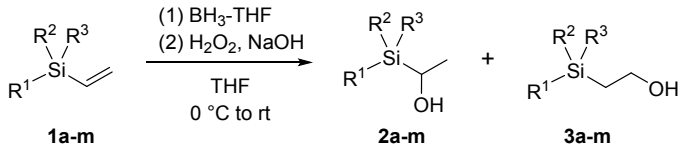

1a-m **2a-m** **3a-m**

Entry	Substrate	R^1	R^2	R^3	Regioisomeric ratio (**2**:**3**)[b]	Isolated yield of **2**[c]	Isolated yield of **3**[c]
1	**1a**	Me	Me	Me	58:42	30%	30%
2	**1b**	Et	Et	Et	61:39	18%	15%
3	**1c**	Me	Me	Ph	63:37	65%	33%
4	**1d**	Me	Ph	Ph	68:32	53%	27%
5	**1e**	Ph	Ph	Ph	71:29	50%	18%
6	**1f**	Me	Me	2-OMe-C_6H_4	55:45	42%	17%
7	**1g**	Me	Me	4-OMe-C_6H_4	62:38	44%	23%
8	**1h**	Me	Me	2-Me-C_6H_4	66:34	60%	23%
9	**1i**	Me	Me	4-Me-C_6H_4	59:41	46%	22%
10	**1j**	Me	Me	2-CF_3-C_6H_4	64:36	50%	24%
11	**1k**	Me	Me	4-CF_3-C_6H_4	68:32	52%	19%
12	**1l**	Me	4-CF_3-C_6H_4	4-CF_3-C_6H_4	68:32	55%	18%
13	**1m**	4-CF_3-C_6H_4	4-CF_3-C_6H_4	4-CF_3-C_6H_4	71:29	43%	16%
14[d]	**1c**	Me	Me	Ph	63:37	N.D.	N.D.
15[e]	**1c**	Me	Me	Ph	<1:>99	N.D.	N.D.

[a] Reaction conditions: 1) borane reagent (2.0 eq.), THF (0.2 M), 2) 30% H_2O_2. aq, 2.0 M NaOH. aq. 0 °C to rt, 2 h. [b] The regioisomeric ratio was determined from the ^{1}H NMR spectra of the crude reaction products. [c] These regioisomers can be separated by silica gel column chromatography. For details please see the Supporting Information. [d] The reaction was conducted using BH_3-Me_2S. [e] The reaction was conducted using 9-BBN. N.D.: Not determined.

.

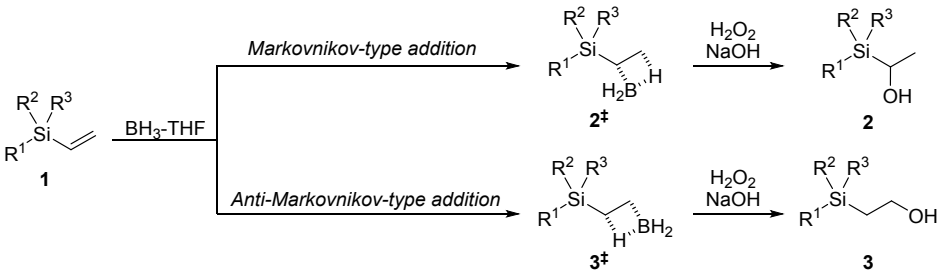

Substrate	$R^1R^2R^3$	G^0(**2**‡) [au]	G^0(**3**‡) [au]	ΔG^0(**2**‡ - **3**‡) [kJ/mol]
1a	Me_3	-513.7616	-513.7617	0.25
1c	Me_2Ph	-705.4527	-705.4523	-1.09
1d	$MePh_2$	-897.1425	-897.1410	-4.01
1e	Ph_3	-1077.0242	-1077.0207	-9.45

Fig. 2. DFT calculation of the hydroboration transition states of **1a**, **1c**, **1d** and **1e**. These values were calculated at the B3LYP/6-31G* level using Spartan'18.

Replacement of methyl group(s) by phenyl group(s) also increased the ratio of 1-silylethanol, namely, the trimethylsilyl substrate (**1a**) gave a ratio of 58:42, whereas the dimethylphenylsilyl (**1c**), methyldiphenyl (**1d**) and triphenylsilyl (**1e**) substrates exhibited ratios of 63:37, 68:32, and 71:29, respectively. To examine the reason for this, we conducted density-functional theory (DFT) calculation of the hydroboration transition states of **1a**, **1b** and **1e**. The calculation condition was set following Xia and coworkers' report.[17] The Markovnikov-type transition state (**2**‡) was increasingly favored over the anti-Markovnikov transition state (**3**‡) as the number of the phenyl group increased ($Me_3 < Me_2Ph < MePh_2 < Ph_3$) (Fig. 2). Thus, the result of DFT calculation was in agreement with the observed regioisomeric ratio of products. In the case of alkynylsilanes, it was reported that the phenyl groups on the silicon atom causes the increase of electrophilicity of the β-carbon atom on the alkynyl group.[18] This electrophilicity of the β-carbon atom is also one possible reason for the order of regioselectivity in the hydroboration of vinylsilanes.

The substituent on the phenyl group(s) only modestly affected the regioisomeric ratio, indicating that such substituents do not significantly affect the electronic state of the vinyl moiety (Table 1). Parks reported that the unique regioselectivity of vinylsilanes arose from both the β-effect of silicon and the reduction of steric hindrance on the α-carbon.[19] Our results suggest that changing the substituents on the silicon atom alters the balance of β-effect and steric effect on the α-carbon only modestly, and therefore both regioisomers are obtained regardless of the silyl functionality.

Development of novel PR ligands

Design and synthesis. With a variety of silylethanols in hand, we next investigated their application as hydrophobic building blocks for biofunctional compounds. As a model target of structural development, we focused on the nuclear progesterone receptor (PR). PR is a member of the nuclear receptor superfamily of ligand-dependent transcription factors regulated by the binding of an endogenous steroid, progesterone (P4).[20-22] PR plays important roles in multiple physiological systems, including female reproductive processes such as uterine cell proliferation and differentiation, the ovulation cycle, and mammary gland growth and differentiation. PR is an attractive target of drug discovery, and several synthetic PR ligands are already in clinical use.[23-25] Hydrophobic interaction is essential for PR ligand activity,[26] and influences the activity mode, namely, agonist or antagonist.[27,28] Thus, we anticipated that application of our silylethanols would be advantageous for the structural development of the hydrophobic moiety in PR ligands. Based on these considerations, we designed novel PR ligand candidates consisting of the silylethoxy moiety as the hydrophobic pharmacophore together with a 3-chloro-4-cyanophenyl group, which serves as a hydrogen-bonding pharmacophore of ligands for PR and related steroid hormone receptors (Fig. 1B).[29,30]

The designed compounds were synthesized by S_NAr reaction of 2-chloro-4-fluorobenzonitrile and silylethanols. Firstly we investigated the conventional S_NAr reaction conditions (NaH in DMF, 80 °C), however, complicated mixtures containing siloxanes were obtained. Therefore, we conducted the reaction using KHMDS as the base reported by Warren.[31] Under this reaction condition, the substrate silylethanols were recovered even though the yield of desired products was low. In the syntheses of methyldiphenylsilyl derivatives **4d-e** and triphenylsilyl derivatives **5d-e**, the reactions with LiHMDS proceeded well, whereas the reactions with KHMDS did not. The yield obtained with the silylethan-1-oxy derivative (α-isomer) was larger than that in the case of the corresponding 2-silylethoxy derivative (β-isomer), especially in the case of bulkier compounds such as triethylsilyl derivatives (**4b** and **5b**), methyldiphenylsilyl derivatives (**4d** and **5d**) and triphenylsilyl derivatives (**4e** and **5e**). This is probably because the silicon atom activates the β-oxyanion to promote the nucleophilic substitution (Tables 2 and 3).

Table 2. Synthesis of designed compounds **4a**-**4e**. [a]

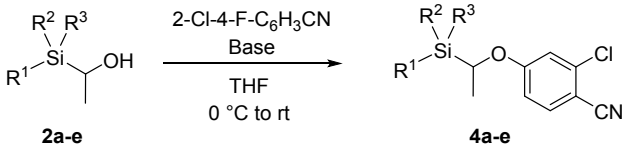

2a-e **4a-e**

Substrate	R^1	R^2	R^3	Base	Product (yield)
2a	Me	Me	Me	KHMDS	**4a** (24%)
2b	Et	Et	Et	KHMDS	**4b** (31%)
2c	Me	Me	Ph	KHMDS	**4c** (22%)
2d	Me	Ph	Ph	LiHMDS	**4d** (62%)
2e	Ph	Ph	Ph	LiHMDS	**4e** (48%)

[a] 2-Chloro-4-fluorobenzonitrile (3.0 eq.), base (2.0 eq.), THF (0.1 M)

Table 3. Synthesis of designed compounds **5a**-**5e**. [a]

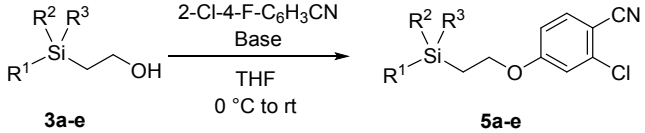

3a-e **5a-e**

Substrate	R^1	R^2	R^3	base	Product (yield)
3a	Me	Me	Me	KHMDS	**5a** (36%)
3b	Et	Et	Et	KHMDS	**5b** (17%)
3c	Me	Me	Ph	KHMDS	**5c** (20%)
3d	Me	Ph	Ph	LiHMDS	**5d** (27%)
3e	Ph	Ph	Ph	LiHMDS	**5e** (14%)

[a] 2-Chloro-4-fluorobenzonitrile (3.0 eq.), base (2.0 eq.), THF (0.1 M)

Evaluation of PR-modulating activity. The PR-modulating activity of the synthesized compounds was assessed by alkaline phosphatase assay using the T47D human breast cancer cell line.[32] PR agonistic activity, i.e., transcription-promoting activity, was assessed after single treatment with the test compounds, and PR antagonistic activity, i.e., transcription-inhibitory activity, was assessed after combination treatment with the test compounds and 1 nM P4. Table 4 summarizes the PR ligand activity of the compounds **4a**-**4e**, **5a**-**5e**. All the synthesized compounds exhibited significant PR ligand potency. Regarding the antagonistic activity, increase of the molecular bulkiness decreased the potency. Among the test compounds, 2-trimethylsilylethoxy derivative **5a** showed the most potent antagonistic activity with an IC_{50} value of 27 nM. Compound **5a** was as potent or more potent than the potent nonsteroidal PR antagonist **6** that we previously developed,[33] indicating that structural development using silylethanols is a promising approach to develop potent new biofunctional compounds. Interestingly, silylethan-1-oxy derivatives (α-isomers) **4a** and **4b** exhibited PR agonistic activity, in contrast to the potent PR antagonistic activity of the corresponding 2-silylethoxy isomers (β-isomers) **5a** and **5b**, indicating that the isomeric structural conversion resulted in activity-switching. Surprisingly, the maximum efficacy of compound **4b** was significantly larger than that of the endogenous PR agonist P4 (Table 4).

Table 4. PR agonistic and antagonistic activities of compounds **4a**-**4e** and **5a**-**5e** assessed by T47D alkaline phosphatase assay.

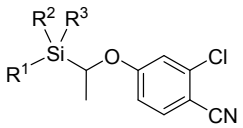

4a-e

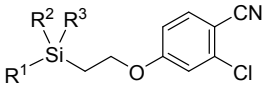

5a-e

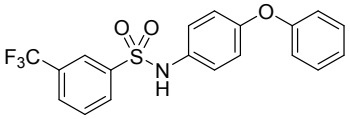

6

Cmpd.	R^1	R^2	R^3	agonist EC_{50} [a] (Emax) [b]	antagonist IC_{50} [c]
4a	Me	Me	Me	620 ± 570 nM (85 ± 38%)	-
4b	Et	Et	Et	110 ± 64 nM (170 ± 70%)	-
4c	Me	Me	Ph	-	33 ± 9 nM
4d	Me	Ph	Ph	-	88 ± 24 nM
4e	Ph	Ph	Ph	-	110 ± 20 nM
5a	Me	Me	Me	-	27 ± 15 nM
5b	Et	Et	Et	-	57 ± 17 nM
5c	Me	Me	Ph	-	34 ± 13 nM
5d	Me	Ph	Ph	-	150 ± 27 nM
5e	Ph	Ph	Ph	-	420 ± 170 nM
6	-			-	33 ± 3 nM

[a] The EC_{50} values are shown as the mean ± SD from three independent experiments. [b] Maximum efficacy compared with the maximum activity of P4. [c] The IC_{50} values are shown as the mean ± SD from three independent experiments. P4 concentration was 1.0 nM.

Docking simulation. To estimate the binding mode of these PR modulators, we conducted docking simulations of triethylsilyl derivatives **4b** (α-isomer), which exhibited agonistic activity, and **5b** (β-isomer), which exhibited potent antagonistic activity, with the X-ray crystal structure of the hPR ligand-binding domain (LBD) (PDB ID: 1A28),[26] using AutoDock 4.2.[34] Compound **4b** has two stereoisomers depending on the chirality of the secondary carbon, and both isomers were docked. Fig. 3A shows the docking model of **4b** as a superimposition of the two isomers on the crystal structure of hPR LBD bound to P4. In the docked structure, the cyano group interacts with Gln725 and Arg766, which interact with the carbonyl group of P4 in the X-ray structure. The triethylsilylethan-1-oxy moiety occupies the hydrophobic cavity of the ligand-binding pocket of the PR LBD in which the CD-ring of P4 is located, forming a hydrophobic interaction with Met909 in helix12 (H12) of PR. It has been reported that the proper folding of Met909 in H12 is essential for the transcriptional activity of PR.[26,35,36] Overall, compound **4b** sufficiently occupies the ligand-binding pocket and forms key interactions with the receptor, enabling it to exert PR agonistic activity. Fig. 3B shows the docking model of **5b** in the hPR LBD. In the docked structure, the cyano group of **5b** interacts with Gln725 and Arg766 in the same manner as in the calculated model of **4b** (Fig. 3). The 2-triethylsilylethoxy group of **5b** occupies a hydrophobic cavity on the contralateral side to the cyanophenyl moiety, similarly to the docked structure of **4b**. In the case of **5b**, however, there is a considerable unoccupied space near Met909, which is occupied by the triethylsilylethan-1-oxy group of **4b**. The lack of hydrophobic interaction might destabilize the proper folding of H12 required for transcriptional activity, and this could be the reason for the activity-switching, namely, whereas **4b** exhibits agonistic activity, **5b** functions as an antagonist (Fig. 3).

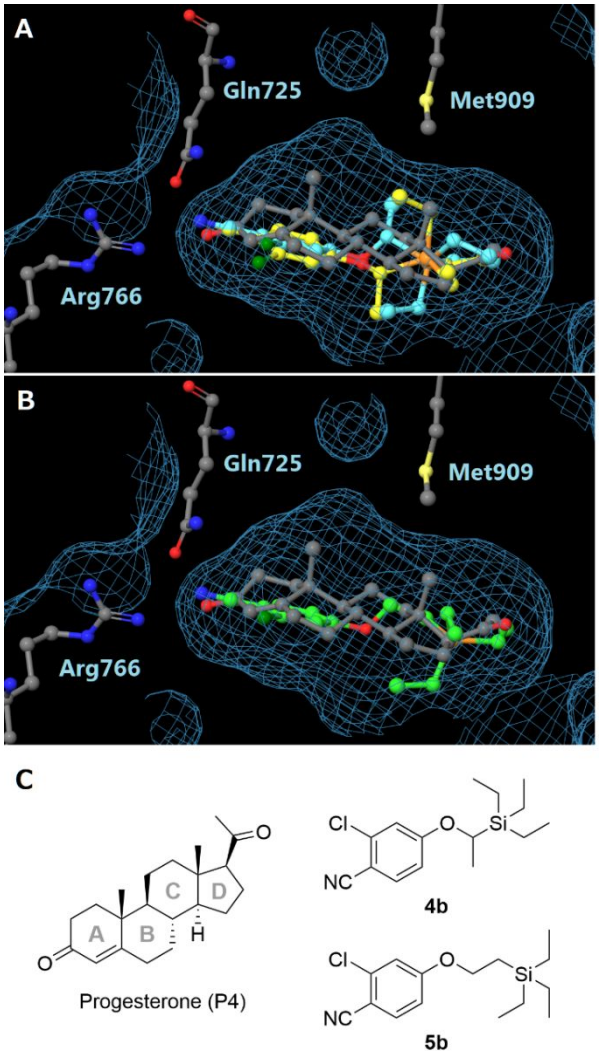

Fig. 3. Docking models of compounds **4b** (α-isomer) and **5b** (β-isomer) with the hPR LBD (PDB ID: 1A28) obtained with AutoDock 4.2. The structure shows the endogenous ligand P4 (gray) bound to the PR LBD, and the docking models of **4b** and **5b** are superimposed. The protein surface is indicated as a blue mesh. A) Superimposition of docking models of the two stereoisomers of **4b** (yellow and light blue) in the hPR LBD. B). Superimposition of the docking model of **5b** (green) on the endogenous ligand P4 (gray). C) Structures of compounds.

Conclusions

To evaluate the characteristic hydroboration reaction profile of vinylsilanes, we investigated the regioisomeric ratio of the hydroboration products of various vinylsilanes. All the investigated vinylsilanes afforded two regioisomers, and an increase in the bulkiness of the silyl functionality increased the proportion of the sterically more hindered α-isomer (Markovnikov products). We then investigated application of the obtained silylethanols to the structural development of nuclear PR modulators. The silylalkoxy moiety proved to be an effective hydrophobic pharmacophore of novel PR antagonists such as **5a** and **5b**. In addition, the isomeric structural conversion of **5a** or **5b**, i.e., to **4a** or **4b**, respectively, resulted in complete activity-switching, namely from antagonist to agonist. These results suggested that silylethanols are useful options for structural development, and that vinylsilanes are a versatile resource for designing hydrophobic building blocks of biofunctional molecules.

Experimental

Chemistry

All reagents were purchased from TCI Chemicals, Fujifilm Wako Pure Chemical Industries, or Kanto Kagaku Co. Inc., and used without further purification: Thin-layer chromatography (TLC) was performed using silica gel coated with a fluorescent indicator F254 (Merck, #1.05715.0001). Silica gel column chromatography was performed using neutral silica gel (60 Å, 40–50 μm) purchased from Kanto Kagaku Co. Inc. NMR spectra were recorded on Bruker Avance 400 (^{1}H: 400 MHz and ^{13}C: 101 MHz), Bruker Avance 500 (^{1}H: 500 MHz and ^{13}C: 126 MHz), and JEOL JNM-GX500 (^{1}H: 500 MHz, ^{13}C: 126 MHz) spectrometers.

Chemical shift values for protons are referenced to the signal of the residual signal chloroform-d (δ 7.26) or acetone-d_6 (δ 2.05), and chemical shift values for carbons are referenced to the carbon resonance of chloroform-d (δ 77.16) or acetone-d_6 (δ 29.84). High-resolution mass (HRMS) spectra were taken on a Bruker Daltonics micrOTOF-2 using the electron spray ionization time-of-flight (ESI-TOF) method. Details of the procedure and the spectra are presented in the Supplementary data

DFT calculations

All density functional theory (DFT) calculations were performed using the Spartan'18 Wavefunction, Inc. Irvine, CA program by the B3LYP method with the 6-31G* basis. The solvent effect was taken into account by using dielectric ratio of THF (7.43) determined by C-PCM model.[37-40] The structure used for energy calculations were confirmed by frequency analysis as transition state (only one imaginary frequency). Previous studies indicate this method is reliable for the study of the hydroboration reaction mechanism.[41-43] Each calculated result was given in Table S1 in supporting information.

T47D alkaline phosphatase assay for the evaluation of the PR antagonistic activity

T47D alkaline phosphatase assays were performed as previously described,[33] with minor modifications. Briefly, the human breast cancer cell line T47D was routinely cultivated in RPMI 1640 medium with 10% FBS at 37 °C in a humidified incubator under 5% CO_2. Cells were plated in 96-well plates and incubated overnight under the same conditions. The next day, the cells were treated with fresh medium containing the test compound in the presence (for antagonist assay) or absence (for agonist assay) of 1 nM progesterone and further incubated for 48 h. The medium was aspirated, and the cells were fixed with 100 µL of 1.8% formalin in phosphate-buffered saline (PBS). The fixed cells were washed with PBS, and 100 µL of assay buffer (1 mg/mL *p*-nitrophenol phosphate in diethanolamine water solution, pH 9.0) was added. The mixture was incubated at room temperature for 2 h under shielding from light. The absorbance was measured at 405 nm using a DTX 880 Multimode Detector (Beckman Coulter). All data points were measured in triplicate, and IC_{50} values were calculated from three independent experiments. EC_{50} values were calculated by sigmoid fitting using a Caleidagraph. IC_{50} values were determined as the concentration of the compound that reduces the P4-induced alkaline phosphatase activity by a half, calculated by linear interpolation from the two points adjacent to the IC_{50} value.

Docking simulation

The structure of the LBD of hPR was prepared from the Protein Data Bank accession number 1A28. Polar hydrogen atoms and partial atomic charges were assigned using AutoDockTools (ADT). Molecular docking was performed using AutoDock 4.2 with the genetic algorithm. The AutoDock parameters for silicon atoms were Rii = 1.60 and eii = 0.875.

Conflicts of interest

There are no conflicts to declare.

Acknowledgements

This work was partially supported by Grants in-Aid for Scientific Research from JSPS (KAKENHI Grant No. 23K06046 (S.F.)), Takeda Science Foundation (S.F.), Hoansha Foundation (S.F.), the Research Center for Biomedical Engineering (S.F.), and JST SPRING under Grant Number JPMJSP2120. (N.N.). This research was also partially supported by AMED under Grant Number JP24ama121043 (Research Support Project for Life Science and Drug Discovery, BINDS). We thank Professor Dr. Masanobu Uchiyama (The University of Tokyo) for helpful discussions about DFT calculations. We also thank Dr. Yosuke Demizu and Dr. Genichiro Tsuji (National Institute of Health Sciences) for kind support for the measurement of mass spectra.

References

1 I. Fleming, A. Barbero and D. Walter, *Chem. Rev.*, 1997, **97**, 2063–2192.
2 E. Langkopf and D. Schinzer, *Chem. Rev.*, 1995, **95**, 1375–1408.
3 R. Richter, G. Roewer, U. Böhme, K. Busch, F. Babonneau, H. P. Martin and E. Müller, *Appl. Organomet. Chem.*, 1997, **11**, 71–106.
4 J. A. Soderquist and S.-J. H. Lee, *Tetrahedro*n, 1988, **44**, 4033–4042.
5 J. O. Bailey and D. A. Singleton, *J. Am. Chem. Soc.*, 2017, **139**, 15710–15723.
6 F. Meng, H. Jang and A. H. Hoveyda, *Chem. Eur. J.*, 2013, **19**, 3204–3214.
7 B. R. Smith, C. M. E. and J. T. Njardarson, *J. Med. Chem.* 2014, **57**, 9764–9773.
8 R. Ramesh and D. S. Reddy, *J. Med. Chem.*, 2018, **61**, 3779–3798.
9 S. Fujii and Y. Hashimoto, *Future Med. Chem.*, 2017, **9**, 485–505.
10 S. Fujii, *Med. Chem. Commun.*, 2016, **7**, 1082–1092.
11 A. K. Franz and S. O. Wilson, *J. Med. Chem.*, 2013, **56**, 388–405.
12 S. Fujii, Y. Miyajima, H. Masuno and H. Kagechika, *J. Med. Chem.*, 2013, **56**, 160–166.
13 D. Kajita, M. Nakamura, Y. Matsumoto, M. Ishikawa, Y. Hashimoto and S. Fujii, *Bioorg. Med. Chem. Lett.*, 2015, **25**, 3350–3354.
14 H. Toyama, M, Nakamura, Y. Hashimoto, S. Fujii, *Bioorg. Med. Chem.*, 2015, **23**, 2982–2988.
15 T. Oikawa, S. Fujii, S. Mori, H. Masuno, K. Emiko and H. Kagechika, *ChemMedChem*, 2022, **17**, 202200176.
16 N. Namba, T. Noguchi-Yachide, Y. Matsumoto, Y. Hashimoto and S. Fujii, *Bioorg. Med. Chem.*, 2022, **66**, 116792.
17 Y. Xia, Y. Li and W. Li, *J. Organomet. Chem.*, 2008, **693**, 3722-3728.
18 K. Igawa and K. Tomooka, *Angew. Chem. Int. Ed.*, 2006, **45**, 232.
19 D. J. Parks and W. E. Piers, *Tetrahedron*, 1998, **54**, 15468–15488.
20 D. J. Mangelsdorf, C. Thummel, M. Beato, P. Herrlich, G. Schütz, K. Umesono, B. Blumberg, P. Kastner, M. Mark, P. Chambon, R. M. Evans, *Cell*, 1995, **83**, 835–839.

21 M. D. Aupperlee, K. T. Smith, A. Kariagina and S. Z. Haslam, *Endocrinology*, 2005, **146**, 3577– 3588.
22 L. Kolatorova, J. Vitku, J. Suchopar, M. Hill and A. Parizek, *Int. J. Mol. Sci.*, 2022, **23**, 7989.
23 D. Africander, N. Verhoog and J. P. Hapgood, *Steroids*, 2011, **76**, 636–652.
24 I. M. Spitz, *Steroids*, 2003, **68**, 981–993.
25 M. S. Islam, S. Afrin, S. I. Jones and J. Segars, *Endocr. Rev.*, 2020, **41**, 1–52.
26 S. P. Williams and P. B. Sigler, *Nature*, 1998, **393**, 392–396.
27 P. Zhang, E. A. Terefenko, A. Fensome, J. Wrobel, R. Winneker, S. Lundeen, K. B. Marschke and Z. Zhang, *J. Med. Chem.*, 2002, **45**, 4379–4382.
28 A. Fensome, W. R. Adams, A. L. Adams, T. J. Berrodin, J. Cohen, C. Huselton, A. Illenberger, J. C. Kern, V. A. Hudak, M. A. Marella, E. G. Melenski, C. C. McComas, C. A. Mugford, O. D. Slayden, M. Yudt, Z. Zhang, P. Zhang, Y. Zhu, R. C. Winneker and J. E. Wrobel, *J. Med. Chem.*, 2008, **51**, 1861–1873.
29 M. Hammond, J. R. Patterson, S. Manns, T. H. Hoang, D. G. Washburn, W. Trizna, L. Glace, E. T. Grygielko, R. Nagilla, M. Nord, H. E. Fries, D. J. Minick, N. J. Laping, J. D. Bray and S. K. Thompson, *Bioorg. Med. Chem. Lett.*, 2009, **19**, 2637–2641.
30 K. Ochiai, R. Yonezawa and S. Fujii, *ChemMedChem*, 2024, **19**, 202400040.
31 S. A. Grecian, S. Hadida and S. D. Warren, *Tetrahedron Lett.*, 2005, **46**, 4683–4685.
32 D. Di Lorenzo, A. Albertini and D. Zava, *Cancer Res.*, 1991, **51**, 4470–4475.
33 A. Yamada, Y. Kazui, H. Yoshioka, A. Tanatani, S. Mori, H. Kagechika and S. Fujii, *ACS Med. Chem. Lett.*, 2016, **7**, 1028–1033.
34 G. M. Morris, R, Huey, W. Lindstrom, M. F. Sanner, R. K. Belew, D. S. Goodsell and A. J. Olson, *J. Comput. Chem.*, 2009, **30**, 2785–2791.
35 I. Petit-Topin, N. Turque, J. Fagart, M. Fay, A. Ulmann, E. Gainer and M.-E. Rafestin-Oblin, *Mol. Pharmacol.*, 2009, **75**, 1317–1324.
36 S. J. Lusher, H. C. A. Raaijmakers, D. Vu-Pham, K. Dechering, T. W. Lam, A. R. Brown, N. M. Hamilton, O. Nimz, R. Bosch, R. McGuire, A. Oubrie and J. de Vlieg, *J. Biol. Chem.*, 2011, **286**, 35079–35086.
37 X. Zhang and J. M. Herbert, *J. Phys. Chem. B*, 2014, **118**, 7806-7817.
38 A. W. Lange and J. M. Herbert, *Chem. Phys. Lett.*, 2011, **509**, 77-87.
39 T. N. Truong and E. V. Stefanovich, *Chem. Phys. Lett.,* 1995, **240**, 253-260.
40 V. Barone and M. Cossi, J. Phys. Chem. A, 1998, **102**, 1995-2001.
41 Y. J. Xu, Y. F. Zhang, and J. Q. Li., *Chem. Phys. Lett.,* 2006, **421**, 36–41.
42 L. Long, X. Lu, F. Tian, and Q. Zhang, J. Org. Chem., 2003, **68**, 4495-4498.
43 D. Liu and Z. Lin, Organometallics, 2002, **21**, 4750–4755.